1

Fundamentals

In this introductory chapter, we review the fundamentals of astrophysical processes that are governed by self-organized criticality (SOC), briefly called "SOC avalanches." We will discover that most complex systems with many interacting components display some nonlinear behavior that is governed by SOC. This book is focused on numerical, analytical, and theoretical modeling of SOC in avalanching astrophysical systems. The major novelty of the described SOC framework is a paradigm shift from *microscopic* cellular automaton simulations to *macroscopic* modeling of physical scaling laws.

The concept of SOC has been pioneered by Per Bak and was first published in the seminal paper by Bak, Tang, and Wiesenfeld (1987), which has been cited already over 4,000 times. A slightly earlier application of SOC is due to Katz (1986). The brief abstract of Bak et al. (1987) succinctly summarizes the quintessence of SOC: "We show that certain extended dissipative dynamical systems naturally evolve into a critical state, with no characteristic time or length scales. The temporal 'fingerprint' of the SOC self-organized critical state is the presence of 1/f noise; its spatial signature is the emergence of scale-invariant (fractal) structure" (Bak et al. 1987). The authors demonstrate the principle of SOC with a simple cellular automaton model, in analogy to the sandpile paradigm (Figure 1.1), which produces avalanches of arbitrary sizes that can be statistically sampled and exhibit a size distribution close to a power law function. The power law shape of size distributions became the hallmark and principal diagnostic of SOC phenomena. However, as we will see in Sections 2.7–2.14, power law distributions are neither necessary nor sufficient conditions for SOC processes. Popular accounts of SOC phenomena can be found in the lucidly written book *How Nature Works* by Bak (1996) and in the article "Self-Organized Criticality" by Bak and Chen (1991). Comprehensive treatments of SOC phenomena can be found in Table 1.2 at the end of this chapter.

https://doi.org/10.1017/9781009562942.004 Published online by Cambridge University Press

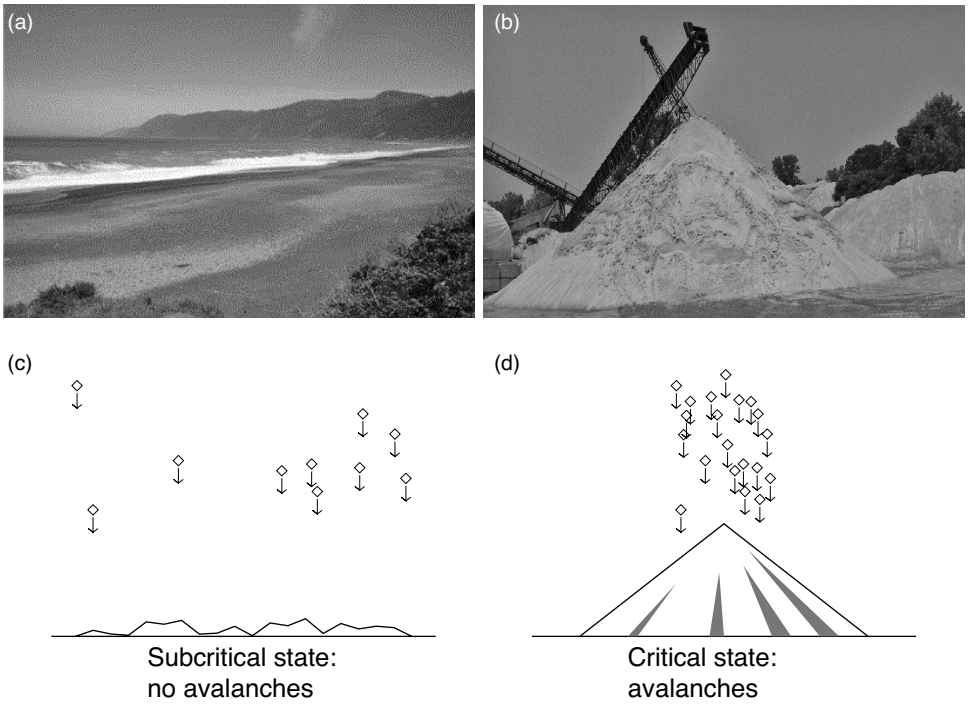


Figure 1.1 A static equilibrium produces no avalanche events (c), such as the flat sand beach in northern California (a), while sand, randomly dripping onto a sandpile, produces a state of SOC, where avalanches occur (d), such as with the conveyer belt of the Indian River Enterprises (b) (Aschwanden 2011a).

1.1 SOC Definitions

The original definition of the term self-organized criticality was inspired by a numerical lattice simulation of a dynamical system with spatially complex patterns, mimicking avalanches of a sandpile, which became the Bak–Tang–Wiesenfeld (BTW) model (Bak et al. 1987), and demonstrated that:

Dynamical systems with extended spatial degrees of freedom naturally evolve into self-organized critical structures of states which are barely stable. Flicker noise, or 1/f noise, can be identified with the dynamics of the critical state. This picture also yields insight into the origin of fractal objects. (Bak et al. 1987)

In this first seminal paper, the authors had already fractal structures such as cosmic strings, mountain landscapes, and coastal lines as potential applications in mind and concluded: *We believe that the new concept of SOC can be taken much further and might be* **the** *underlying concept of dissipative systems with extended degrees of freedom* (Bak et al. 1987). In this spirit, the application of the SOC concept has been broadened substantially over the last 38 years.

https://doi.org/10.1017/9781009562942.004 Published online by Cambridge University Press

If we read a recent definition of SOC, we find:

Self-organized criticality is regarded as scale invariance without external tuning of a control parameter, but with all the features of the critical point of an ordinary phase transition, in particular long range (algebraic) spatio-temporal correlations (Pruessner 2012).

Another definition of SOC can be gleaned from *Wikipedia*:

In physics, self-organized criticality is a property of (classes of) dynamical systems which have a critical point as an attractor. The macroscopic behavior thus displays the spatial and/or temporal scale-invariance characteristic of the critical point of a phase transition, but without the need to tune control parameters to precise values.

In the same vein, it is stated in the original paper of the SOC creators: *The criticality in our theory is fundamentally different from the critical point at phase transitions in equilibrium statistical mechanics, which can be reached by tuning of a parameter, for instance the temperature* (Bak et al. 1987). The aspect of self-tuning in SOC systems is the most crucial difference to (second-order) phase transitions, where fine-tuning is necessary and is not automatically arranged by nature. The implications and theoretical details of this peculiar feature are discussed in Watkins et al. (2016). However, whenever there is a threshold for instabilities, the threshold value itself could be called a "critical point" that decides whether an instability, also called a nonlinear energy dissipation event, or avalanche, happens or not. Over the past 38 years, a lot of applications of the SOC concept have been made to slowly driven systems with a critical threshold, especially in solar and astrophysics, which is studied in this book. We therefore like to use a more pragmatic and empirical definition of SOC systems, as depicted in Figure 1.2:

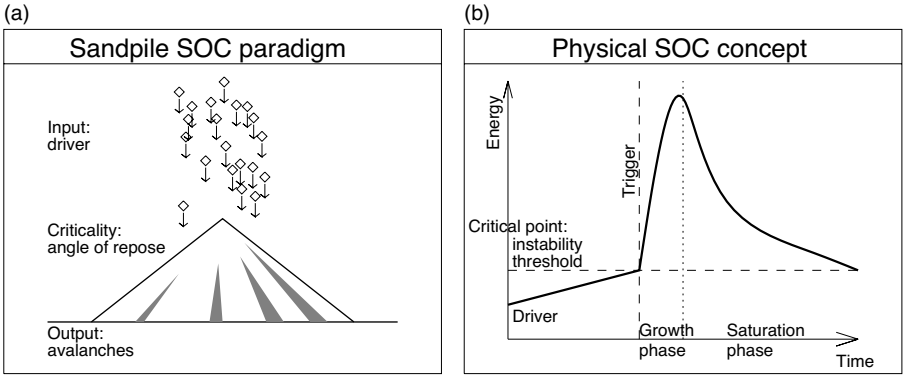


Figure 1.2 (a) The original sandpile SOC paradigm, consisting of the (input) driver, the SOC mechanism (self-tuning angle of repose), and the (output) avalanches. (b) In a physical SOC concept, the driver is a slow and continuous energy input rate, the criticality mechanism is replaced by a critical point in form of a global instability threshold, where an avalanche is triggered, usually consisting of a nonlinear growth phase and a subsequent saturation phase (Aschwanden et al. 2016).

https://doi.org/10.1017/9781009562942.004 Published online by Cambridge University Press

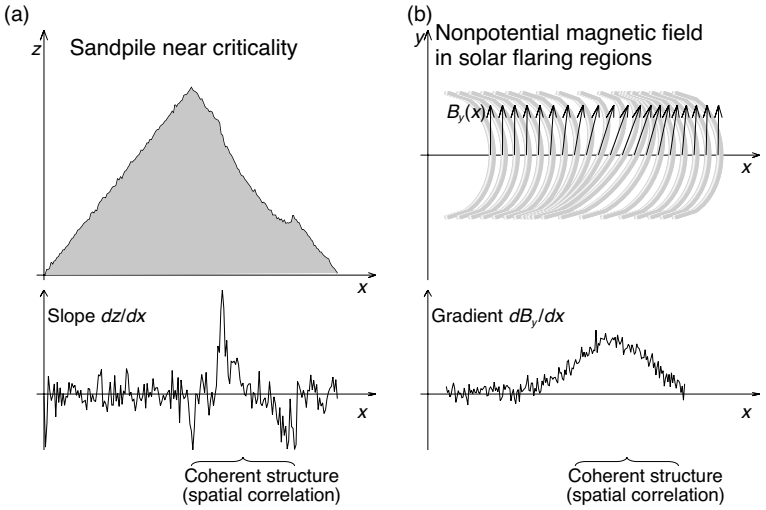


Figure 1.3 (a) A sandpile in a SOC state in the vicinity of criticality is shown in terms of a vertical component $z(x)$, with the slope (or repose angle) dz/dx (bottom), exhibiting short-range fluctuations due to noise, and long-range correlations due to local deviations from the mean critical slope. (b) The analogy of a solar flaring region is visualized in terms of a loop arcade straddling along a neutral line in x-direction, consisting of loops with various shear angles that are proportional to the gradient of the field direction B_x/B_y, showing some local (nonpotential) deviations from the potential magnetic field (bottom) (Aschwanden et al. 2016).

SOC is a critical state of a nonlinear energy dissipation system that is slow and continuously driven toward a critical value of a system-wide instability threshold, producing scale-free, fractal-diffusive, and intermittent avalanches with power law-like size distributions. (Aschwanden 2014)

With this definition, we broaden the meaning of the term "criticality" to a more general meaning of a "critical point," which includes almost any nonlinear system with a (global) instability threshold, such as gravity (Figure 1.3a) or a magnetic field (Figure 1.3b). In addition, a SOC system has to be self-organizing or self-tuning without an external control parameter, which is accomplished by a *slow and continuous driver* and brings the system back to the critical point after each avalanche. Thus, we can say that a SOC system has energy balance between the slowly driven input and the (spontaneously) avalanching output, and thus energy is conserved in the system (in the time average).

1.2 SOC Drivers

The driver is the input part of a SOC system. Without a driver, avalanching would die out and the system becomes subcritical and static (Figure 1.1a). On the other side, the driver must be slowly and continuous, so that the critical state is restored in

https://doi.org/10.1017/9781009562942.004 Published online by Cambridge University Press

the asymptotic limit, while a strong driver would lead the system into a catastrophic collapse and may destroy the system. In the classical BTW model, sand grains are dripped under the action of gravity at a slow rate, at random locations of the sandpile, which refill and restore dents from previous avalanches toward the critical angle of repose (Figure 1.3a).

In astrophysical systems (Table 1.1), the driver or energy input of a SOC system may be gravity (in galaxy formation, star formation, black holes, planet formation, and asteroid formation), gravitational disturbances (in Saturn ring), or creation and stressing of magnetic flux (Figure 1.3b) (in solar flares, stellar flares, neutron stars, and pulsar glitches). The driver must bring the system back to the critical point after each major avalanche, which means that the system is locally pushed toward the instability threshold again, so that further avalanching can occur. In the slowly driven limit, the time duration of an avalanche is shorter than the (waiting) time intervals between two subsequent events, which warrants a separation of time scales. In some natural systems, the driver may temporarily or permanently stop, such as the solar dynamo during the Maunder minimum, which stopped solar flaring. Likewise, the final stage of the sweep-up of debris, left over from the formation of the solar system 4.0 billion years ago, stopped lunar cratering.

An overview of terrestrial SOC phenomena (top half of Table 1.1), astrophysical SOC phenomena (bottom half of Table 1.1), drivers that provide a steady energy input (second column in Table 1.1), instability thresholds at the critical state (third column in Table 1.1), and energy dissipation in form of intermittent avalanches (right column in Table 1.1), are juxtaposed in Table 1.1. In summary, SOC drivers discussed here include gravity fields, magnetic fields, mechanical stress forces, biological growth, chemical reactions, as well as randomly dripping of sand grains.

1.3 Instability and Criticality

We broaden the meaning of "criticality" in the original BTW model to a system-wide "instability threshold," which does not need to be tuned by external parameters, since an "instability threshold" is established by common physical conditions throughout a system. For instance, an earthquake is triggered at a critical stressing break point that may have a similar threshold in different tectonic plates around the globe, due to similar geophysical conditions (i.e., the gravity force at the same distance from Earth center, similar continental drift rates, rock constitutions, and crust fracturing conditions). In analogy, a magnetic instability leading to magnetic reconnection is caused by similar physical threshold conditions in solar active regions (such as the kink instability, the torus instability, or the tearing mode instability), and thus solar or stellar flares occur whenever such global instability thresholds are exceeded locally. Such instabilities occur naturally because the driver brings the

https://doi.org/10.1017/9781009562942.004 Published online by Cambridge University Press

Table 1.1 *Hypothetical physical mechanisms operating in self-organized criticality systems.*

Phenomenon	Energy input (steady driver)	Instability threshold (criticality)	Energy output (intermittent avalanches)
SOC-related systems:			
Sandpile	Gravity (dripping sand)	Angle of repose	Sand avalanches
Superconductor	Magnetic field change	Phase transition	Vortex avalanches
Ising model	Temperature increase	Phase transition	Atomic spin-flip
Tea kettle	Temperature increase	Boiling point	Vapor bubbles
Earthquakes	Tectonic stressing	Dynamical friction	Rupture area
Forest fire	Tree growth	Fire ignition point	Burned area
BTW cellular automaton	Random nodes	Critical threshold	Next-neighbor redistribution
Astrophysics:			
Lunar craters	Meteorite production	Lunar collision	Lunar impact craters
Asteroid belt	Planetesimals	Critical mass density	Asteroid
Saturn ring	Gravitational disturbances	Collision rate	Saturn ring particles
Magnetospheric substorm	Solar wind	Magnetic reconnection	Auroral bursts
Radiation belt	Solar wind	Magnetic trapping	Electron bursts
Solar flares	Magnetic stressing	Magnetic reconnection	Nonthermal particles
Stellar flares	Magnetic stressing	Magnetic reconnection	Nonthermal particles
Pulsar glitches	Neutron star spin-up	Vortex unpinning	Neutron starquakes
Soft gamma-ray repeaters	Magnetic stressing	Star crust fracture	Neutron starquakes
Black-hole objects	Gravity	Accretion and inflow	X-ray bremsstrahlung pulses
Blazars	Quasar jets	Jet direction jitter	Optical radiation pulses
Cosmic rays	Galactic magnetic fields	Acceleration threshold	High-energy particles

https://doi.org/10.1017/9781009562942.004 Published online by Cambridge University Press

system continuously back to the instability threshold. In sandpiles, the dripping of additional sand grains rises the angle of repose wherever it is subcritical. In earthquakes, the continental drift is continuously driven by forces that are rooted below the Earth crust. In solar flares, differential rotation, emergence of magnetic flux, and braiding of magnetic fields by random motion in the subphotospheric magnetoconvection layer continuously build up nonpotential free magnetic energy that can be released in subsequent avalanches. The analogy of unstable coherent structures in a near-critical state in sandpiles and solar flares is visualized in Figure 1.3.

A selection of plasma instabilities that have been theoretically modeled and identified in astrophysical phenomena is shown in Figure 1.4. These instabilities are controlled by gravitational, hydrodynamic, and magneto-hydrodynamic (MHD) forces. Although the geometric and spatiotemporal structures of these (plasma) instabilities are quite different from case to case, they share common dynamic characteristics, such as an exponentially growing phase (after exceeding a system-wide threshold), followed by a saturation phase, which we will use to calculate scaling laws between the underlying physical parameters. In our avalanche scenario, the duration of an avalanche is commensurable with the exponential-growth time, and the peak value of a time profile is an approximate measure of the dissipated energy in an avalanche event (Figure 1.2).

1.4 Avalanching

Avalanches are defined as nonlinear energy dissipation events, which occur in our generalized SOC definition whenever and wherever a local instability threshold is exceeded. Avalanches are the output part of a SOC system, which balance the energy input rate in the time average for conservative SOC systems. Avalanches are detectable events, which can be obtained in astrophysical observations with large parameter statistics, such as obtained from their observed length scales (L), time scales or durations (T), fluxes (F), and fluences or energies (E). The occurrence frequency distributions of these observables tend to be power law-like functions, a hallmark of SOC systems, but deviations from power law functions can be explained by measurement bias effects (such as incomplete sampling, finite system-size effects, and truncations of distributions) or could reflect multiple physical processes. Unnecessary to say that these observables and their size distributions and underlying scaling laws provide important tests of SOC models.

The time evolution of avalanches contains essential information on the underlying spatiotemporal transport process (i.e., diffusion, fractal diffusion, percolation, turbulence, etc.). A generic time evolution is an initially nonlinear (i.e., exponential) growth phase (Figure 1.2b), followed by a quenching or saturation phase (as expressed in the popular saying "No tree grows in the sky!"). In solar flares,

https://doi.org/10.1017/9781009562942.004 Published online by Cambridge University Press

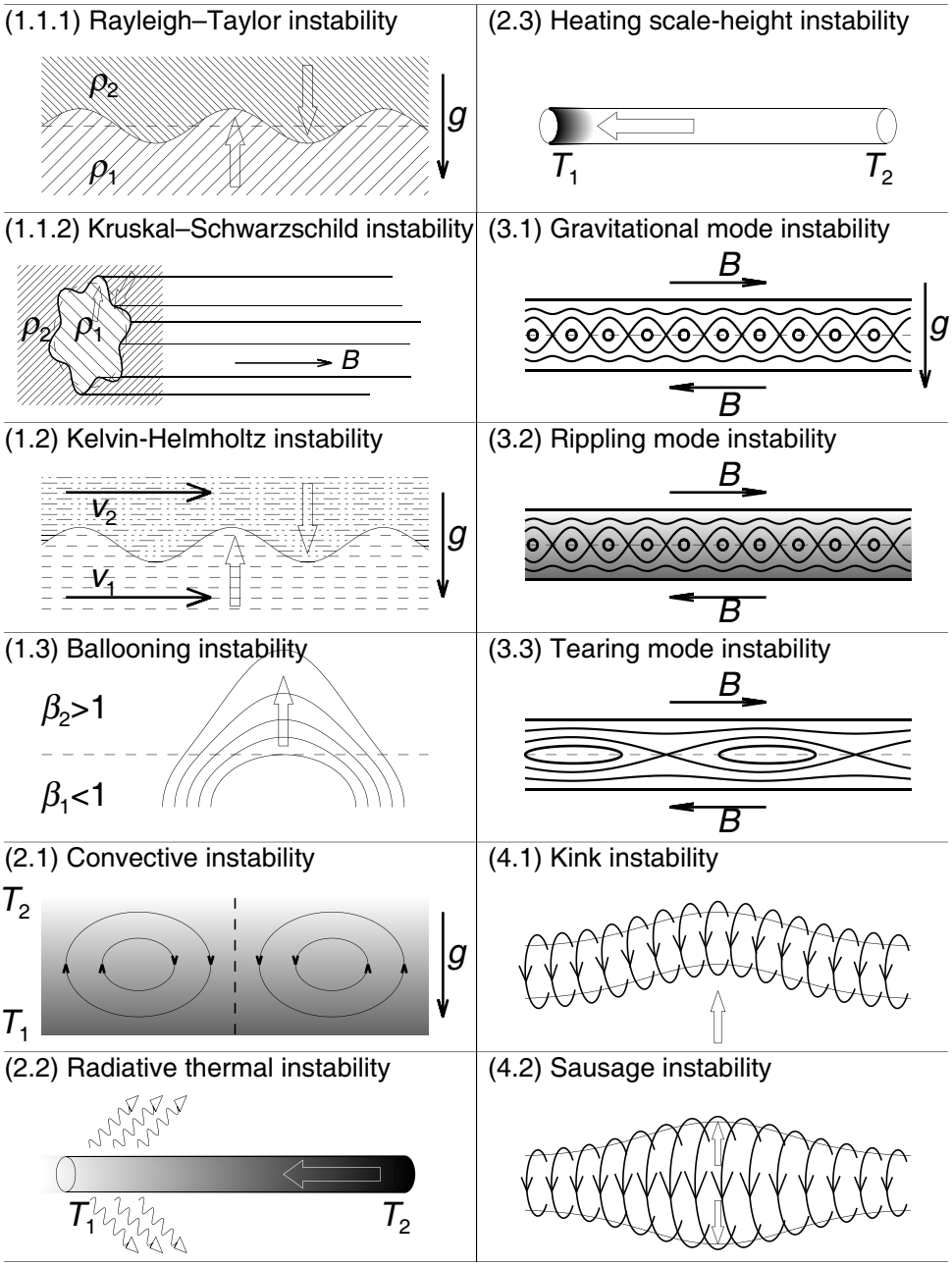


Figure 1.4 Hydrodynamic and MHD instabilities that can occur in plasma physics are illustrated. Different densities (ρ_1, ρ_2) are rendered with hatched linestyle, different velocities (v_1, v_2) with dashed linestyle, temperature gradients (T_1, T_2) with grayscales, longitudinal magnetic field lines (B_0) with thin solid lines, azimuthal magnetic field components (B_φ) with thick solid lines, and radiation with wiggly lines. The directions of the disturbances that lead to an instability are indicated with thick white arrows (Aschwanden 2004).

https://doi.org/10.1017/9781009562942.004 Published online by Cambridge University Press

the initial growth phase is called "impulsive phase," and the subsequent saturation phase is called "postflare phase." In earthquakes, the terms "precursors" and "after-shocks" are common.

1.5 Microscopic Structure

Self-organized criticality systems are a means to study complexity, systems with extended degrees of freedom. Ultimately, a real-world object consists of as many degrees of freedom as the Avogadro number of atoms, that is, $N_A = 6.0 \times 10^{23}$. Such large numbers prevent us from modeling complex nonlinear systems in a deterministic way. In order to deal with SOC systems, we have to resort to numerical simulations with far fewer degrees of freedom, and we have to approximate the complexity of microscopic structures by macroscopic parameters and statistical probability distributions. For example, the complex microscopic structure of the solar chromosphere (Figure 1.5a,) can be rendered with a binary lattice on a much coarser scale (Figure 1.5b). The question is, whether the basic physics that governs the dynamics of a real-world system can also be adequately represented by numerical lattice simulations. In the example shown in Figure 1.5, one binary node of a lattice corresponds to a cube with 1,000-km length scale on the solar surface,

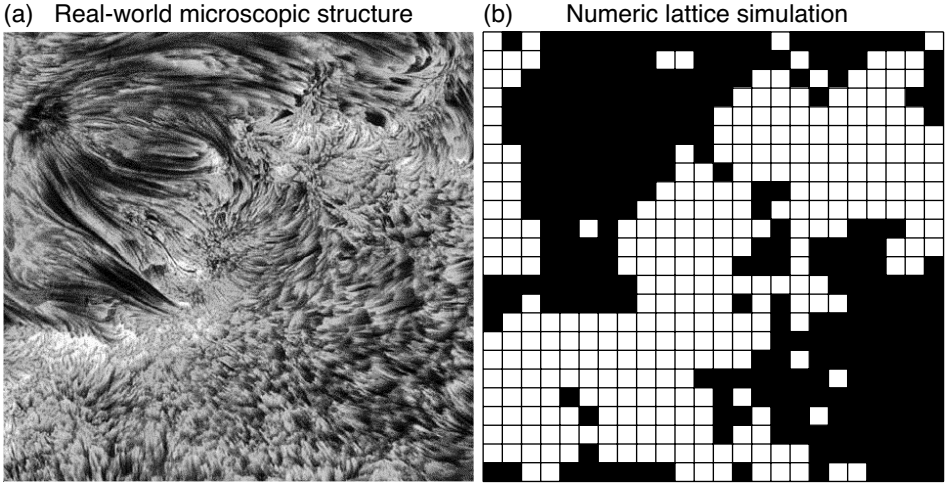


Figure 1.5 (a) A high-resolution image (480 × 480 pixel) of chromospheric spicules in solar active region 10380, observed on 2003, June 16, with the Swedish 1-m Solar Telescope (SST) on La Palma, Spain, using a tunable filter, tuned to the blue-shifted line wing of the Hα 6536 Å line (Courtesy of Bart De Pontieu). (b) A digitized binary (two-level) version of the left solar image is shown, using a lattice grid with a size of 24 × 24 nodes (or cells). The left image shows the microscopic structure of real-world data, while the right image shows the rendering of numerical lattice simulations used in SOC models (Aschwanden et al. 2016).

https://doi.org/10.1017/9781009562942.004 Published online by Cambridge University Press

where the complex plasma dynamics driven by MHD processes exceeds the information content of a binary lattice node by far, so that it appears to be hopeless to mimic the dynamics of a SOC system with numerical cellular automaton simulations. Interestingly however, numerical lattice simulations do reproduce the emergent complex behavior in physical systems to some extent, regardless of the vast discrepancy of spatial scales and information content. For instance, the statistical size distribution of solar flares can be reproduced with cellular automatons for various physical parameters (spatial, temporal scales, flux, and energy), as demonstrated by Lu and Hamilton (1991). Therefore, SOC models have the powerful ability to give us insight into system dynamics in complex systems, regardless of the intricate details of real-world microscopic fine structure. On the other side, the mathematical world of numerical lattice simulations created a whole new cosmos of complex spatial patterns (i.e., Wolfram 2002) and cellular automaton toy models (Pruessner 2012), which appear to have nothing in common with real-world microscopic fine structure, except that they provide practical means to simulate the same dynamic behavior of complex nonlinear systems. Consequently, in this text on solar and astrophysical SOC applications, the emphasis is not on mathematical and numerical SOC models (except when they were specifically designed for astrophysical applications), although they dominate the extant SOC literature.

1.6 Scale-Free Probability

Common characterizations of SOC systems are statistical distributions of SOC parameters (also called "size distributions," "occurrence frequency distributions," or "log(N)-log(S) plots"). How do we derive a statistical *probability distribution function* for SOC systems? This question has been answered in the original SOC papers (Bak et al. 1987, 1988) in an empirical way, by performing numerical Monte Carlo simulations of avalanches in Cartesian lattice grids, according to the well-known algorithm with next-neighbor interactions (BTW model). Several theoretical attempts have been made to derive statistical probabilities, by considering avalanches as a branching process (Christensen and Olami 1993), by exact solutions of the Abelian sandpile (Dhar and Ramaswamy 1989; Dhar 1999; Dhar and Majumdar 1990), by considering the BTW cellular automaton as a discretized diffusion process using the Langevin equations (Wiesenfeld et al. 1990; Zhang 1989), or by renormalization group theory (Pietronero et al. 1994; Vespignani et al. 1995; Loreto et al. 1995). Most of these analytical theories represent special solutions to a particular set of mathematical redistribution rules but predict different power law exponents for the probability distribution functions obtained with each method, and thus lack the generality to interpret the ubiquitous and omnipresent SOC phenomena observed in nature.

https://doi.org/10.1017/9781009562942.004 Published online by Cambridge University Press

A simple approach to estimate the size distributions of SOC avalanche sizes has recently been proposed by making a simple statistical probability argument, called the *scale-free probability conjecture* (Aschwanden 2012a, 2014, 2015), which predicts the functional form of power laws for most observable SOC parameters, and predicts specific values for their power law slopes (or exponents). The derivation goes as follows. If we consider the derivation of a normal or Gaussian distribution function, we can toss a number of dice and enumerate all possible statistical outcomes, ending up with a binomial distribution function, which converges to a Gaussian distribution function for a large number of dice, and thus characterizes a maximum likelihood distribution. Similarly, we can enumerate all statistically possible sizes L of avalanches in a system bound by a finite size L_{max}, which is simply a number density that is reciprocal to the volume $V = L^d$ of avalanches with size L, that is,

$$N(L)dL \propto L^{-d}dL \qquad \text{for } L \leq L_{max}, \tag{1.1}$$

where d is the Euclidean dimension of the SOC system, having values of $d = 1$, 2, or 3. Figure 1.6 illustrates how the number of 1-D, 2-D, and 3-D avalanches (approximated by spheres) increases reciprocally with the size of the avalanches. This distribution function is based on the principle of statistical maximum likelihood, which follows from braking up a finite system volume into smaller pieces. This distribution function is also related to *packing rules* (e.g., sphere packing) in geometric aggregation problems. A similar approach using geometric scaling laws was also applied to earthquakes (Main and Burton 1984). Of course, for slowly driven SOC systems, only one avalanche happens at a time, and thus the whole SOC system is not fully "packed" with avalanches occurring at once, but the statistical likelihood probability for an avalanche of a given size is nevertheless proportional to the packing density, for a statistically representative subset of all possible avalanche sizes (in a system with $L \leq L_{max}$). This basic scale-free probability conjecture (Eq. 1.1) straightforwardly predicts the size distribution of length scales of SOC avalanches, namely, $N(L) \propto L^{-3}$ in 3-D space, and can be used to derive the size distributions of other geometric parameters.

1.7 Fractal Geometry

"Fractals in nature originate from self-organized critical dynamical processes" (Bak and Chen 1989). The fractal geometry has been postulated for SOC processes by the first proponents of SOC. However, the geometry of fractals has been explored about a decade earlier than the SOC concept (Mandelbrot 1977, 1983, 1985). An extensive discussion of measuring the fractal geometry in SOC systems associated with solar and planetary data is given in Aschwanden (2011a, chapter 8) and McAteer (2013).

https://doi.org/10.1017/9781009562942.004 Published online by Cambridge University Press

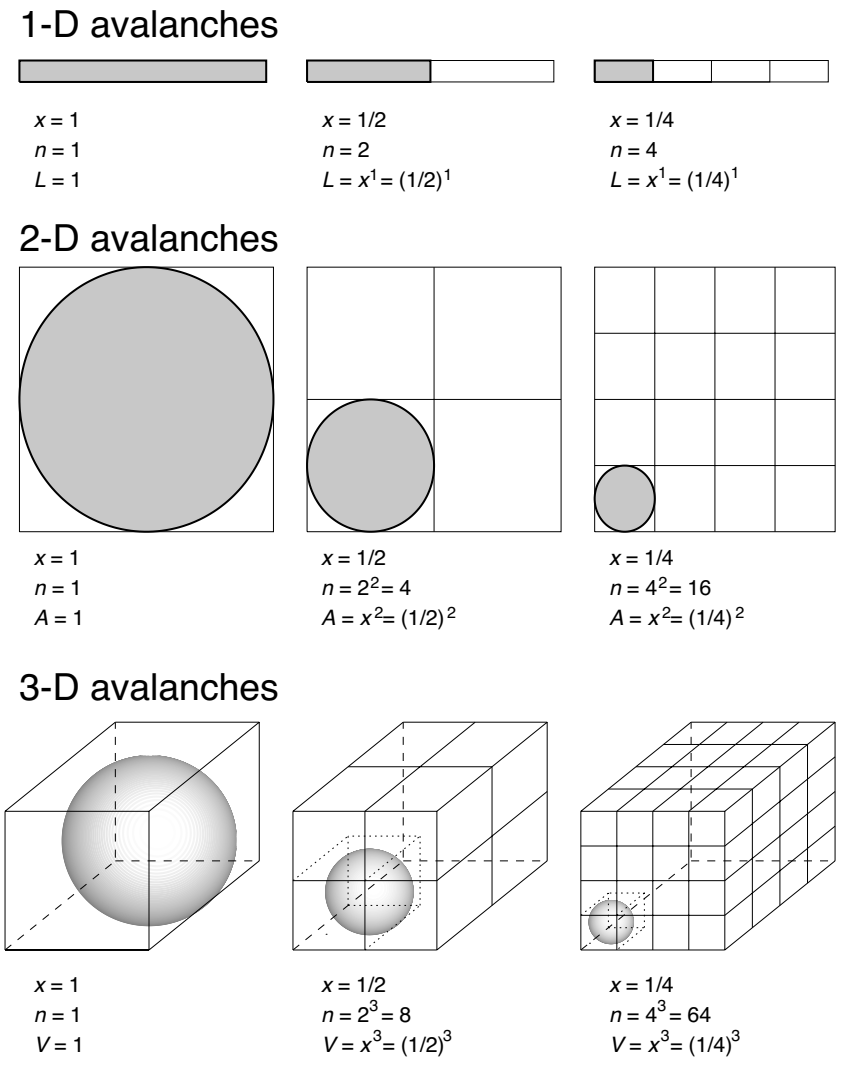


Figure 1.6 Schematic diagram of the Euclidean volume scaling of spherical avalanches, visualized in the three Euclidean space dimensions $d = 1, 2, 3$. The Euclidean length scale x of subcubes decreases by a factor 2 in each step ($x_i = 2^{-i}$, $i = 0, 1, 2$), while the number of subcubes increases by $n_i = (2^i)^d$, defining a probability of $N(x_i) \propto x_i^{-d}$ for each avalanche size with size x_i (Aschwanden 2012a).

The simplest fractal is the Hausdorff dimension D_d, which is a monofractal and depends on the Euclidean space dimension $d = 1, 2, 3$. The Hausdorff dimension D_V for the 3-D Euclidean space ($d = 3$) is

$$D_V = \frac{\log V_f}{\log (L)}, \tag{1.2}$$

https://doi.org/10.1017/9781009562942.004 Published online by Cambridge University Press

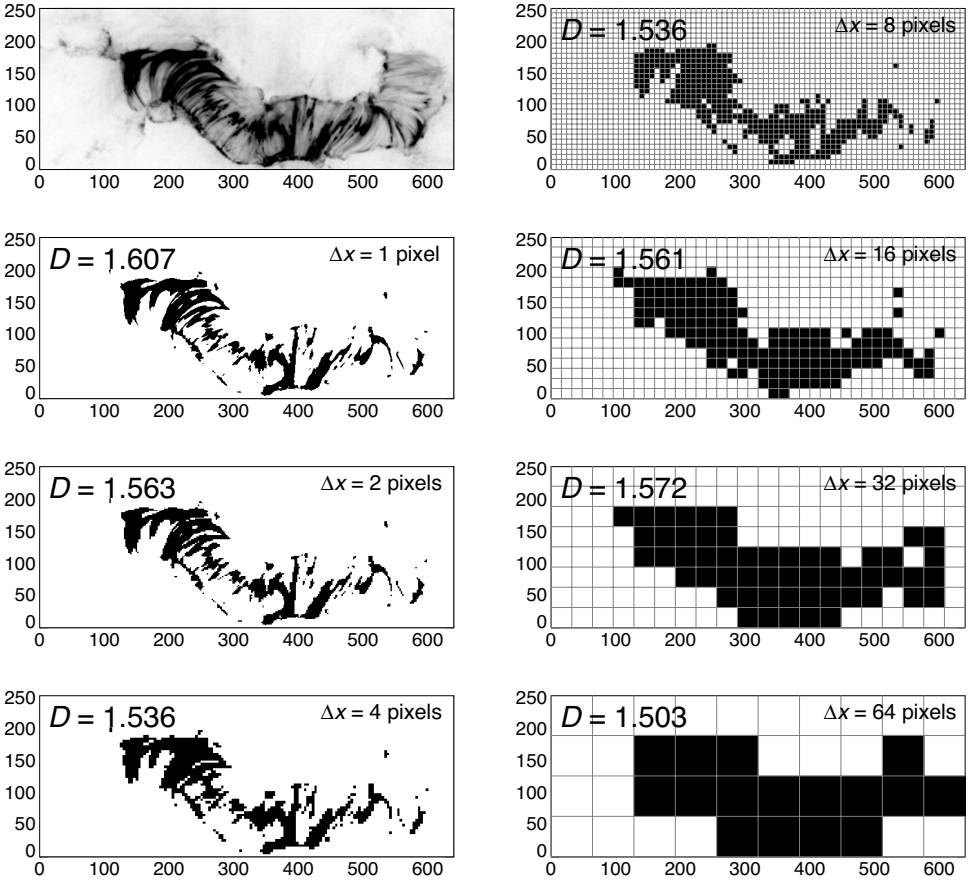


Figure 1.7 Measurement of the fractal area of a solar flare, observed by TRACE 171 Å on 2000, Jul 14, 10:59:32 UT. The Hausdorff dimension is evaluated with a box-counting algorithm for pixels above a threshold of 20% of the peak flux value, yielding a mean of $D_A = 1.55 \pm 0.03$ for the seven different spatial scales ($\Delta x = 1, 2, 4, \ldots, 64$ pixels) shown here (Aschwanden and Aschwanden 2008a, 2008b).

and analogously for the 2-D Euclidean space ($d = 2$),

$$D_A = \frac{\log A_f}{\log (L)}, \tag{1.3}$$

with A_f and V_f being the fractal area and volume of a SOC avalanche. These fractal dimensions can be determined by a box-counting method, where the area fractal D_A can readily be obtained from images of the real world (e.g., for a solar flare as shown in Figure 1.7), while the fractal volume D_V is generally not available (except in numerical simulations), unless one infers the corresponding 3-D information from stereoscopic triangulation or tomography. A good approximation for the

https://doi.org/10.1017/9781009562942.004 Published online by Cambridge University Press

expected fractal dimension D_d of SOC avalanches is the mean value of the smallest possible fractal dimension $D_{d,min} \approx (d-1)$ and the largest fractal dimension $D_{d,max} = d$, that is,

$$D_d \approx \frac{D_{d,min} + D_{d,max}}{2} = d - \frac{1}{2}. \tag{1.4}$$

Thus, we expect a mean fractal dimension of $D_V = 2.5$ for the 3-D space and $D_A = 1.5$ for the 2-D space. The example shown in Figure 1.7 yields a value of $D_A = 1.55 \pm 0.03$, which is close to the theoretical prediction $D_A = 1.50$ for $d = 2$ in Eq. (1.4). As a footnote, this new definition of the minimum fractal dimension $D_{d,min} = (d-1)$ is slightly different from the earlier definition $D_{d,min} = 1$ in Aschwanden (2012a), but they are identical for $d = 2$.

Fractals are measurable from the spatial structure of an avalanche at a given instant of time. Therefore, they enter the statistics of time-evolving SOC parameters, such as the observed flux or intensity per time unit, which is proportional to the number of instantaneous active nodes in a lattice-based SOC avalanche simulation.

1.8 Spatiotemporal Evolution

Let us consider some basic aspects in the time domain of SOC avalanches. The spatiotemporal evolution of SOC avalanches has been simulated with cellular automaton simulations (Bak et al. 1987, 1988; Lu and Hamilton 1991; Charbonneau et al. 2001), which produced statistics of the final avalanche sizes L and time durations T, but there is virtually no statistics on the spatiotemporal evolution of the instantaneous avalanche size or radius $r(t)$ as a function of time t, which could characterize the macroscopic transport process. Statistics on this spatiotemporal evolution is important to establish spatiotemporal correlations and scaling laws between L and T, which defines the macroscopic transport process.

Ignoring the complexity of the microscopic transport, which is quantified by an iterative redistribution rule in cellular automaton simulations, we can measure the radius $r(t) = \sqrt{A(t)/\pi}$ of a circular 2-D area $A(t)$ as a function of time t, which corresponds to the solid (Euclidean) area that is equivalent to the time-integrated fractal avalanche area. This has been performed for BTW cellular automaton simulations (Aschwanden 2012a), as well as for solar flare data (Aschwanden 2012b; Aschwanden and Shimizu 2013; Aschwanden et al. 2013b), and was found to fit a diffusion-type relationship,

$$r(t) = \kappa (t - t_0)^{\beta/2}, \tag{1.5}$$

where t_0 is the onset time of the instability, κ is the diffusion coefficient, and β is the diffusive spreading exponent: A value of $\beta \lesssim 1$ corresponds to subdiffusion, $\beta = 1$

https://doi.org/10.1017/9781009562942.004 Published online by Cambridge University Press

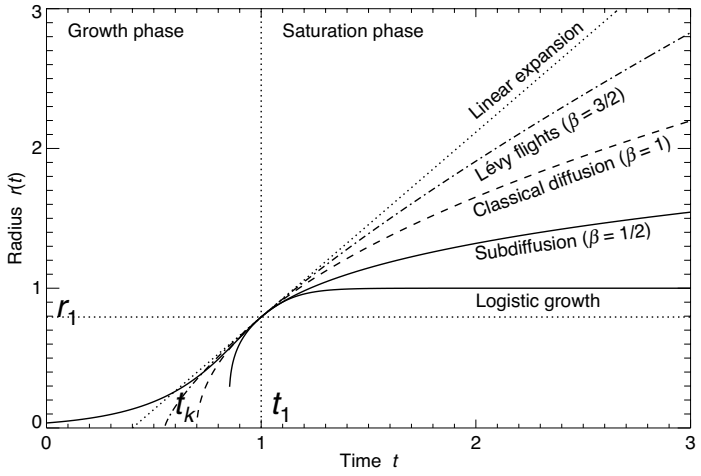


Figure 1.8 Comparison of spatiotemporal evolution models: Logistic growth with parameters $t_1 = 1.0, r_\infty = 1.0, \tau_G = 0.1$, subdiffusion ($\beta = 1/2$), classical diffusion ($\beta = 1$), Lévy flights or hyper-diffusion ($\beta = 3/2$), and linear expansion ($r \propto t$) (Aschwanden 2012a).

to classical diffusion, $\beta \gtrsim 1$ to hyper-diffusion or Lévy flight, and $\beta = 2$ to linear expansion (Figure 1.8). From this macroscopic evolution, we expect a statistical scaling law of the form,

$$L \propto T^{\beta/2}, \tag{1.6}$$

for the final sizes L and durations T of SOC avalanches. Substituting this scaling law $L(T)$ (Eq. 1.6) into the probability distribution function $N(L)$ of length scales L (Eq. 1.1), we establish a power law distribution function for time scales,

$$N(T)dT = N(L[T])\frac{dL}{dT}dT = T^{-[1+(d-1)\beta/2]}\,dT = T^{-\alpha_T}\,dT, \tag{1.7}$$

with the power law slope of

$$\alpha_T = 1 + \frac{(d-1)\beta}{2}, \tag{1.8}$$

which has a value of $\alpha_T = 2.0$ for 2-D Euclidean space ($d = 2$) and a value of $\alpha_T = 1.5$ for 2-D Euclidean space ($d = 2$). This power law slope for avalanche time scales is a prediction of universal validity, since it is only based on the scale-free probability conjecture (Eq. 1.1), $N(L) \propto L^{-d}$, and the statistical property of random walk (or classical diffusion) in the transport process.

The transport process in avalanching systems is found to be diffusion-dominated in systems with extremely strong perturbations (Bregman 2007).

https://doi.org/10.1017/9781009562942.004 Published online by Cambridge University Press

1.9 Flux–Volume Scaling

The original BTW model specifies avalanche sizes by the total number of active nodes, which corresponds to the cluster area of an avalanche in a 2-D lattice. If we want to characterize the area $a(t)$ of an avalanche as a function of time, which is a highly fluctuating quantity in time, we can define also a time-integrated final area $a(< t)$ that includes all nodes that have been gone unstable at least once during the course of an avalanche, which is a monotonically increasing quantity and quantifies the size of an avalanche with a single number $A = a(t = T)$, which we simply call the time-integrated avalanche area.

In real-world data, we observe a signal from a SOC avalanche in form of an intensity flux $f(t)$ (e.g., seismic waves from earthquakes, hard X-ray flux from solar flares, or the amount of dissipated magnetic energy in a solar flare. Let us assume that this intensity flux is proportional to the volume of active nodes in the BTW model, which corresponds to the instantaneous fractal volume $V_f(t)$ (Eq. 1.2) in a macroscopic SOC model (Aschwanden 2012a, 2014, 2015),

$$f(t) \propto V_f(t) \propto r(t)^{D_d}. \tag{1.9}$$

The flux time profile $f(t)$ is expected to fluctuate substantially in real-world data as well as in lattice simulations, because the approximation of the instantaneous volume of a SOC avalanche implies a highly variable fractal dimension $D_d(t)$, which can vary in the range of $D_{d,min} \approx (d-1)$ and $D_{d,max} = d$, with a mean value $D_d = (d - 1/2)$ (Eq. 1.4). Occasionally, the instantaneous fractal dimension may reach its maximum value, that is, $D_d(t) \lesssim d$, which defines an expected upper limit $f_{max}(t)$,

$$f_{max}(t) \propto V(t) \propto r(t)^{d}. \tag{1.10}$$

This is an important quantity that corresponds to the peak flux $f_{max}(t)$ of an avalanche, which is often measured in astrophysical observations.

1.10 Coherent and Incoherent Radiation

Self-organized criticality models can be diagnosed and tested by means of statistical distributions, for example, by the omnipresent power law or power law-like size distributions, and by the underlying scaling laws that relate the power law slopes of different observables to each other (see also McAteer et al. 2016 for a description of methods). The original paradigm of a SOC model, the BTW cellular automaton simulations (Bak et al. 1987, 1988), produce power law distributions of two variables, the size S, and the time duration T. The size S is simply defined by the time-integrated area A of active nodes (pixels) in 2-D lattice simulations, or by the time-integrated fractal volume V_f of active nodes (voxels) in 3-D lattice simulations.

https://doi.org/10.1017/9781009562942.004 Published online by Cambridge University Press

In astrophysical observations, however, the volume of an avalanche cannot be measured directly, but rather a flux intensity F_λ in some wavelength regime λ is observed, which is not necessarily proportional to the fractal volume V_f, depending on the emission mechanism that is dominant at wavelength λ. Therefore, for astrophysical observations in particular, we have to introduce a relationship between the observed flux F_λ and the emitting volume V_f that is fractal for a SOC avalanche process. For sake of simplicity we characterize this relationship with a power exponent γ (Aschwanden 2012b),

$$F_\lambda \propto (V_f)^\gamma. \tag{1.11}$$

This definition allows us to distinguish two categories of physical processes: *incoherent processes* that have a linear relationship between the emitting flux and volume ($\gamma = 1$) and *coherent processes* that have a nonlinear relationship ($\gamma > 1$),

$$F_\lambda \propto (V_f)^\gamma, \qquad \begin{cases} \gamma > 1 & \text{(coherent process)} \\ \gamma = 1 & \text{(incoherent process)} \end{cases} \tag{1.12}$$

Incoherent processes are, for instance, free–free emission in optically thin plasma, bremsstrahlung, or gyrosynchrotron emission. Free–free emission is a common emission mechanism in soft X-rays and EUV, where the total flux scales with the emission measure EM and is integrated over the entire (fractal) source volume V_f. Coherent processes on the other hand, can occur by wave–particle interactions in collisionless plasmas, such as loss-cone instabilities, electron-beam instabilities, or microwave amplification by stimulated emission of radiation (MASER) emission. The flux level of coherent waves amplifies exponentially or with a nonlinear power to the spatial scale of the source and thus with a nonlinear power to the source volume.

1.11 Separation of Time Scales

Most of the original numerical simulations of SOC systems were performed in the slowly driven limit, which warrants a strict separation of time scales. In lattice-type cellular automaton simulations, the separation of time scales is enforced by dropping only one single sand grain at a time, or disturbing only one single lattice node at a time. If nothing happens, the algorithm proceeds with the next input of a disturbance. In the alternative case, when a disturbance triggers an avalanche, the incremental input function is stopped until the avalanche process ends, after which another input step is continued. This asymptotic limit of strict time-scale separation between the waiting time scale and durations of subsequent avalanches is also called a "slowly-driven SOC system." This ideal, but unnatural condition is, however, not necessarily always enforced in nature. Especially for SOC systems with time-variable drivers, the trigger rate can get so high that multiple avalanches are

https://doi.org/10.1017/9781009562942.004 Published online by Cambridge University Press

triggered near-simultaneously and small avalanches occur at various places while a previously triggered large avalanche is still evolving. If we encounter such a "multi-avalanching system," or multi-avalanching behavior during some busy periods of time, we may call it a "fast-driven" or "strongly driven" system. We can adopt the terminology of a slow or fast driver as a synonym for the existence or nonexistence of time-scale separation, which can be expressed by the ratio of the avalanche duration T to the waiting time τ,

$$\begin{array}{rl} \text{Slow driver}: & \mapsto \ \tau \gtrsim T \\ \text{Fast driver}: & \mapsto \ \tau \lesssim T \end{array} . \tag{1.13}$$

For a fast driver, the question arises how this affects the observed (power law-like) size distributions that we calculate in the slowly driven limit. The answer depends very much on the event detection method. Ideally one would use imaging information so that the spatial locations of two temporally overlapping events can be separately determined and the time profiles of the two events can be properly disentangled. In practice, especially in the case of astrophysical observations, spatial sources of co-temporaneous events cannot be resolved and a time-series analysis is the only available method. In that case, superimposed time profiles of different events can still be separated if they have a characteristic shape, for instance, a rapid rise and an exponential decay, using a deconvolution method. If no proper deconvolution method is applied, which is unfortunately the case in almost all published studies with event statistics applied to SOC models, there will be a systematic bias of underestimating the time duration of long events, especially when the rule is applied that a previous event has to end before the next event is detected. This leads predictably to steeper power law slopes in the time-scale distribution $N(T)$. We will see later on that an increase in the event rate (for instance, the flaring rate during the maximum of the solar cycle) will lead to substantially steeper power law slopes of the time-scale duration (for solar flare events detected in soft X-rays), from a value of $\alpha_T \approx 2$ in the slowly driven regime (during solar cycle minimum) to a large value of $\alpha_T \lesssim 5$ in the fast-driven regime (during solar cycle maximum). Interestingly, the size distribution of fluxes was not affected in the slowly driven regime. In another study, it was demonstrated that low-resolution observations of a time profile causes an exponential cutoff at large values of the time-scale distribution, which also leads to steeper power law slopes (Isliker and Benz 2001). Thus, we generally expect steeper power laws or exponential distributions of time scales in the limit of strong driving with clustered events that violate the separation of time scales, although there are also reports with flatter power law slopes during episodes of higher event rates (e.g., Bai 1993; Georgoulis and Vlahos 1996, 1998).

https://doi.org/10.1017/9781009562942.004 Published online by Cambridge University Press

1.12 Universality of SOC

About 38 years ago, the concept of SOC emerged (Bak et al. 1987), initially envisioned to explain the ubiquitous 1/f-power spectra, which can be characterized by a power law spectrum $P(\nu) \propto \nu^{-1}$. The term *1/f power spectra* or *flicker noise* should actually be understood in broader terms, including power spectra with pink noise ($P(\nu) \propto \nu^{-1}$), red noise ($P(\nu) \propto \nu^{-2}$), and black noise ($P(\nu) \propto \nu^{-3}$), essentially everything except white noise ($P(\nu) \propto \nu^{0}$). While white noise represents traditional random processes with uncorrelated fluctuations, 1/f power spectra are a synonym for time series with nonrandom structures that exhibit long-range correlations. These nonrandom time structures represent the avalanches in Bak's paradigm of sandpiles. Consequently, Bak's seminal paper in 1987 triggered a host of numerical simulations of sandpile avalanches, which all exhibit power law-like size distributions of avalanche sizes and durations. These numerical simulations were, most commonly, cellular automatons in the language of complexity theory, which are able to produce complex spatiotemporal patterns by iterative application of a simple mathematical redistribution rule. The numerical algorithms of cellular automatons are extremely simple, basically a one-liner that defines the lattice redistribution rule, with an iterative loop around it, but can produce the most complex dynamical patterns, similar to the beautiful geometric patterns created by Mandelbrot's fractal algorithms (Mandelbrot 1977, 1983, 1985). An introduction and exhaustive description of cellular automaton models that simulate SOC systems is given in Pruessner (2012), and a review of cellular automaton models applied to solar physics is given in Charbonneau et al. (2001).

Four years after introduction, Bak's SOC concept was applied to solar flares, which were known to exhibit similar power law size distributions for hard X-ray peak fluxes, total fluxes, and durations as the cellular automaton simulations produced for avalanche sizes and durations (Lu and Hamilton 1991). This discovery enabled a host of new applications of the SOC concept to astrophysical phenomena, such as solar and stellar flare statistics, magnetospheric substorms, X-ray pulses from accretion disks, pulsar glitches, and so forth. A compilation of SOC applications to astrophysical phenomena is given in a recent textbook (Aschwanden 2011a), as well as in recent review articles (Aschwanden 2013b; Aschwanden et al. 2016; Crosby 2011). The successful spreading of the SOC concept in astrophysics mirrored the explosive trend in other scientific domains, such as the application of SOC in magnetospheric physics (auroras, substorms; Sharma et al. 2016), in geophysics (earthquakes, mountain and rock slides, snow avalanches, forest fires; Hergarten 2002), in biophysics (evolution and extinctions, neuron firing, spread of diseases), in laboratory physics (Barkhausen effect, magnetic domain patterns, Ising model, tokamak plasmas; Jensen 1998), financial physics (stock market

https://doi.org/10.1017/9781009562942.004 Published online by Cambridge University Press

crashes; Sornette 2004), and social sciences (urban growth, traffic, global networks, internet) or sociophysics (Galam 2012). This wide range of applications elevated the SOC concept to a truly interdisciplinary research area, which inspired Bak's vision to explain "how nature works" (Bak 1996). What is common to all these systems is the statistics of nonlinear processes, which often ends up in power law-like size distributions. Other aspects that are in common among the diverse applications are complexity, contingency, and criticality (Bak and Paczuski 1995), which play a grand role in complexity theory and systems theory. Feedback plays a very important role in the phenomena of SOC, as it ensures a steady state, where the system is marginally stable against a disturbance (Kadanoff 1989).

What became clear over the last 38 years of SOC applications is the duality of (i) an universal statistical aspect and (ii) a special physical system aspect. The universal aspect is a statistical argument that can be formulated in terms of the scale-free probability conjecture (Aschwanden 2012a), which explains the power law function and the values of the power law slopes of most occurrence frequency distributions of spatiotemporal parameters in avalanching systems. This statistical argument for the probability distributions of nonlinear systems is as common as the statistical argument for binomial or Gaussian distributions in linear random systems. In this sense, solar flares, earthquakes, and stock market systems have a statistical commonality (e.g., de Arcangelis et al. 2006). On the other hand, each SOC system may be governed by different instabilities that are unique to each observed SOC phenomenon, such as plasma magnetic reconnection physics in solar flares, mechanical stressing of tectonic plates in earthquakes, or the networking of brokers in stock market crashes. So, one should always be aware of this duality of model components when creating a new SOC model. There is no need to reinvent the universal statistical aspects or power law probability distributions each time, while the modeling of physical systems may be improved with more accurate measurements and model parameterizations in every new SOC application.

There is another duality in the application of SOC: the numerical world of lattice simulation toy models and the real world of quantitative observations governed by macroscopic physical laws. The world of lattice simulations has its own beauty in producing complexity with mathematical simplicity, but it cannot capture the physics of a SOC system. It can be easily designed, controlled, modified, and visualized. It allows us to perform Monte Carlo simulations of SOC models and may give us insights about the universal statistical aspects of SOC. Real-world phenomena, in contrast, need to be observed and measured with large statistics and reliable parameters that have been cleaned from systematic bias effects, incomplete sampling, and unresolved spatial and temporal scales, which is often hard to achieve. However, computer power has increased drastically over the last 38 years, exponentially according to Gordon Moore's law, so that enormous databases with

https://doi.org/10.1017/9781009562942.004 Published online by Cambridge University Press

up to $\approx 10^9$ events have been gathered per dataset from some SOC phenomena, such as from solar small-scale phenomena for instance (McIntosh and Gurman 2005).

1.13 SOC Textbooks and Reviews

At the time of writing we count at least 18 textbooks related to the topic of SOC, which are listed in Table 1.2 in chronological order. The titles of these textbooks reflect the early interest in fractals, before SOC concepts came "en vogue."

Besides the text book references, the topic of SOC is also well documented with over 37 reviews (at the time of writing). However, there is no review that

Table 1.2 *Textbooks on the topic of SOC.*

Book title	References
The Fractal Geometry of Nature	Mandelbrot (1977)
Fractals	Feder (1988)
Fractals, Chaos, Power Laws: Minutes from an Infinite Paradise	Schroeder (1991)
How Nature Works: The Science of Self-Organized Criticality	Bak (1996)
Self-Organized Criticality: Emergent Complex Behavior in Physical and Biological Systems	Jensen (1998)
Cellular Automatons	Ilachinski (2001)
Self-Organized Criticality in Earth Systems	Hergarten (2002)
Discovery of Cosmic Fractals	Baryshev and Teerikorpi (2002)
Critical Phenomena in Natural Sciences: Chaos, Fractals, Self-Organization and Disorder: Concepts and Tools	Sornette (2004)
The Nonlinear Universe: Chaos, Emergence, Life	Scott (2007)
Lectures in Supercomputational Neuroscience: Dynamics in Complex Brain Networks	BeimGraben et al. (2008)
Theory of Zipf's Law and Beyond	Saichev et al. (2009)
Self-Organized Criticality in Astrophysics. The Statistics of Nonlinear Processes in the Universe	Aschwanden (2011a)
Self-Organised Criticality: Theory, Models and Characterisation	Pruessner (2012)
Sociophysics: A Physicist's Modeling of Pseudo-Political Phenomena	Galam (2012)
Self-Organized Criticality Systems	Aschwanden, ed. (2013b)
Natural Complexity: A Modeling Handbook	Charbonneau (2017)
Complexity Physics	Jensen (2023)

https://doi.org/10.1017/9781009562942.004 Published online by Cambridge University Press

covers all interdisciplinary fields and aspects of SOC sciences. Nevertheless, the partial reviews cover SOC in a nutshell (Nagler et al. 1999; p. 516 in Aschwanden 2019); natural complexity (Bak and Paczuski 1995; Watkins and Freeman 2008; Sanchez and Newman 2018; Newman 2011; Toledo-Roy et al. 2019); the issue of how nature works (Raup 1997; Bhattacharya 1997; Bak and Weissman 1997; Finnigan 2001; Buchanan 2015; Watkins et al. 2016); geophysics (Turcotte 1999; Sachs et al. 2013; Hergarten 2013a); forest fires (Clar et al. 1996; Hergarten 2013b); networks (Zou et al. 2013); computer simulations (Pruessner 2013); percolation models (Milovanov 2013); fractals (McAteer 2013; McAteer et al. 2016); ecology (Kelty-Stephen et al. 2013); branching processes (Corral and Font-Clos 2013); turbulence (Vlahos and Isliker 2016); solar flares (Charbonneau et al. 2001; Charbonneau 2013; Crosby 2013); space and laboratory plasma (Sharma et al. 2016); and astrophysics (Aschwanden 2013b, 2013c; Aschwanden et al. 2016; Turolla et al. 2015).

1.14 Summary

Self-organized criticality (SOC) is a theoretical concept that describes the statistics of nonlinear processes. It is a fundamental principle that is common to many nonlinear dissipative systems in the universe. Due to its universality and ubiquity, SOC is a law of nature, for which we derive the theoretical framework and specific macroscopic physical models in this book. The SOC concept was introduced by Bak, Tang, and Wiesenfeld in 1987 and has been applied to laboratory experiments of sandpiles, to human activities such as population growth, language, economy, traffic jams, or wars, to biophysics, geophysics (earthquakes, landslides, forest fires), magnetospheric physics, solar physics (flares), stellar physics (flares, cataclysmic variables, accretion disks, black hole object, pulsar glitches, gamma ray bursts), and to galactic physics and cosmology. From an observational point of view, the hallmark of SOC behavior is the power law shape of occurrence frequency distributions of spatial, temporal, and energy scales, implying scale-free nonlinear processes. Power laws are neither a necessary nor a sufficient condition for SOC behavior, because intermittent turbulence produces power law-like size distributions also. A novel trend that is ongoing in current SOC research is a paradigm shift from "microscopic" scales (in numerical cellular automaton simulations) toward "macroscopic" modeling based on physical scaling laws.

https://doi.org/10.1017/9781009562942.004 Published online by Cambridge University Press